Geomechanics and Engineering, *Vol. 37, No. 3 (2024) 293-306*
https://doi.org/10.12989/gae.2024.37.3.293

Research on the deformation characteristics and support methods of the cross-mining roadway floor influence by right-angle trapezoidal stope

Zhaoyi Zhang[1,2] and Wei Zhang*[3]

[1]*State Key Laboratory of the Gas Disaster Detecting, Preventing and Emergency Controlling, Chongqing 400037, China*
[2]*CCTEG Chongqing Research Institute, Chongqing 400037, China*
[3]*School of Architecture and Engineering, Liaocheng University, Liaocheng 252000, China*

(*Received April 20, 2023, Revised March 29, 2024, Accepted April 29, 2024*)

Abstract. Influenced by the alternating effects of dynamic and static pressure during the mining process of close range coal seams, the surrounding rock support of cross mining roadway is difficult and the deformation mechanism is complex, which has become an important problem affecting the safe and efficient production of coal mines. The paper takes the inclined longwall mining of the 10304 working face of Zhongheng coal mine as the engineering background, analyzes the key strata fracture mechanism of the large inclined right-angle trapezoidal mining field, explores the stress distribution characteristics and transmission law of the surrounding rock of the roadway affected by the mining of the inclined coal seam, and proposes a segmented and hierarchical support method for the cross mining roadway affected by the mining of the close range coal seam group. The research results indicate that based on the derived expressions for shear and tensile fracture of key strata, the ultimate pushing distance and ultimate suspended area of a right angle trapezoidal mining area can be calculated and obtained. Within the cross mining section, along the horizontal direction of the coal wall of the working face, the peak shear stress is located near the middle of the boundary. The cracks on the floor of the cross mining roadway gradually develop in an elliptical funnel shape from the shallow to the deep. The dual coupling support system composed of active anchor rod support and passive U-shaped steel shed support proposed in this article achieves effective control of the stability of cross mining roadways, which achieves effective control of floor by coupling active support and preventive passive support to improve the strength of the surrounding rock itself. The research results are of great significance for guiding the layout, support control, and safe mining of cross mining roadways, and to some extent, can further enrich and improve the relevant theories of roof movement and control.

Keywords: cross mining roadway; right angle trapezoidal stope; short distance coal seam; stress distribution; zoning support

1. Introduction

The activity of the overlying strata in the cross mining roadway generally plays a key control role in the stability of the surrounding rock. Various theoretical hypotheses have been proposed regarding the characteristics of overlying rock activity in mining areas and the stress transmission mechanism of surrounding rocks (Wang *et al*. 2019, Wang *et al*. 2021, He *et al*. 2018, Zhang *et al*. 2023). The representative ones are the cantilever beam hypothesis, articulated rock block hypothesis, transfer rock beam theory, and masonry beam model, as well as the theoretical calculation methods for roof settlement and support load derived based on the above theoretical models. There are significant differences in the characteristics of rock pressure behavior between irregular roof stopes and long wall regular roof stopes, and research is needed on the determination method, combination effect, and mechanical model of key strata of irregular roof (Yang *et al*. 2019, Wu *et al*. 2023). The expression of stress distribution under different mining distances was obtained considered the pressure in the goaf, the gravity of the overlying rock, and the constraint conditions (Ma *et al*. 2022). The identification method and fracture mechanism of key strata and combination key strata in shallow coal seams were studied, and the theory of shallow key strata was proposed (Zhang *et al*. 2021). The high-level thick and hard roof was simplified into a mechanical model of thin roof under different boundary conditions, and the ultimate span drop distance considering the influence of horizontal stress was obtained (Zhao *et al*. 2021). The irregular shape of the working face was proposed as the direct reason for the significant deviation between the measured value of the pressure step and the numerical simulation and theoretical calculation value (Xiong *et al*. 2024).

The current research results mainly focus on simplifying the key strata in rectangular mining areas into long beams or thin plates, and on this basis, a relatively basic mechanical analysis has been conducted on the bending characteristics of irregular key strata. The dynamic prediction model was established for the stability of stope roof by combining on-site detection and similarity simulation methods with engineering geological conditions (Liu *et al*. 2021). A mechanical model was established for the distribution of roof pressure in inclined coal seam mining roadway (Shan *et al*. 2021). The thin plate theory

*Corresponding author, Dr.
E-mail: zhangw@lcu.edu.cn

ISSN: 2005-307X (Print), 2092-6219 (Online)

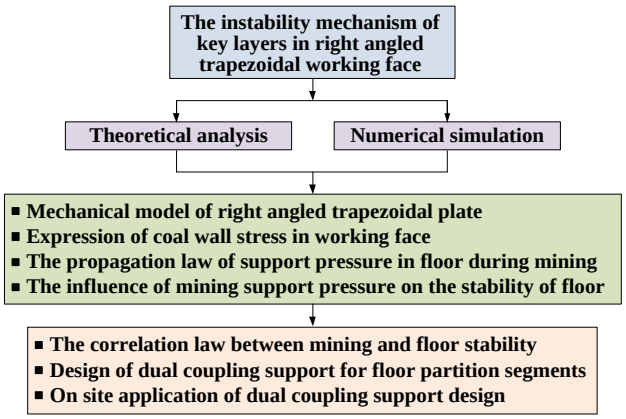

Fig. 1 Support ideas of cross mining roadways affected by right angled trapezoidal working face

was used to analyze the fracture mechanism of the overlying strata in steep dip mining and the basic stress distribution characteristics of the overlying strata when the roof is fractured in upward mining (Yang *et al*. 2024). The existing research results have preliminarily established a mechanical model for the key strata structure of the roof, providing a preliminary reference basis for the safe mining of long wall working faces (Meng *et al*. 2023, Pan *et al*. 2022, Liu *et al*. 2023). However, the theoretical research on inclined trapezoidal mining areas still lags behind the roof control in trapezoidal mining areas (Wen *et al*. 2023). Therefore, theoretical research on the fracture characteristics and stress transfer mechanism of irregular roof slabs still needs to be further explored.

In order to solve the problem of stability control of surrounding rock of cross mining roadway, the design method of bolt support parameters was analyzed for structural stability of cross mining roadway by using fuzzy cluster analysis method (Wang *et al*. 2020). The instability characteristics of the roadway floor under high level stress conditions was studied through numerical simulation and proposed preventive measures for non-uniform support in key areas (Xu *et al*. 2019). The grouting U-shaped steel support anchor cable coupling support technology scheme was proposed (Tian *et al*. 2024). The range of roadway loosening zone was conducted in-depth research on, improving the bearing capacity of surrounding rock, and the coupling characteristics between surrounding rock and support, which played a positive role in the reasonable parameter design of anchor bolts and the stability control of surrounding rock (Chen *et al*. 2022). In order to reduce the deformation of the bottom bulge in deep underground soft rock roadways, the three-dimensional fast Lagrangian analysis method was used to analyze four support design modes (Wang *et al*. 2021).

The above research simplifies roof collapse as an ideal overall cutting model, explores the impact, stress distribution, and stress transfer characteristics of roof collapse, and provides a theoretical basis for quantitative analysis of cross mining roadway support. However, the focus of its prevention and control is mostly on a single coal and rock mass medium, and there is no systematic establishment of a roadway support system under the dynamic activity characteristics of the overlying strata. This article focuses on the mechanism of overlying rock movement in trapezoidal mining areas under inclined coal seam mining face adjustment conditions and the support characteristics of close distance cross mining roadways. The correlation characteristics and mechanical criteria between overlying rock structure movement and roadway surrounding rock failure are studied. By revealing the disturbance mechanism of surrounding rock stress peak under mining influence, a segmented directional control method for cross mining roadways is proposed.

2. Analysis of roof breaking in irregular stopes

2.1 Mechanical model of trapezoidal key strata

To analyze the deformation characteristics and support methods of cross mining roadways affected by right angled trapezoidal working face, takes the inclined longwall mining of the 10304 working face of Zhongheng coal mine as the engineering background (Fig. 1). Zhongheng coal mine is located in Liupanshui, China, with geographic coordinates of 104°29′51″-104°30′16″E and 26°02′22″-26°02′59″N. The inclination angle of the 3 coal seam where the cross-mining face 10304 is located is 33° on average, which is an inclined coal seam (Fig. 2). The thickness of the 3 coal seam where cross-mining face 10304 is located varies greatly, the coal thickness is 1.5-2.5 m. The direct roof is light greenish gray siltstone and fine sandstone with horizontal wave shape and intermittent horizontal lamination. The direct roof of the coal seam is siltstone, with hard, dense lithology and laminae development. The direct floor is gray mudstone, and the lithology has the characteristic of becoming soft when encountering water (Table 1). The failure forms of the surrounding rock are manifested as floor bulge, roof settlement, and cracking of the sides. The amount of floor bulge reaches 300-500 mm, and the amount of roof settlement reaches 100-200 mm.

The working face of 10304 is a typical right-angle trapezoidal mining face, and the beveled edge is the advancing direction of the working face. the lower part of the working face of 10304 is the transport roadway, and the

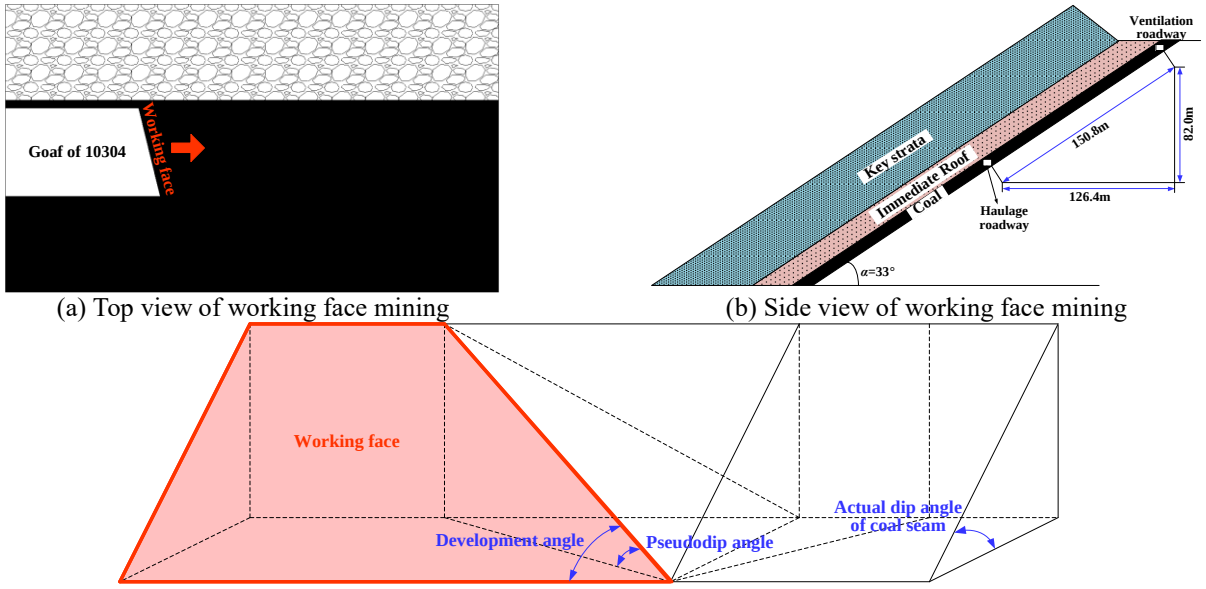

(a) Top view of working face mining (b) Side view of working face mining

(c) Schematic diagram of working face mining

Fig. 2 Design diagram of 10304 working face

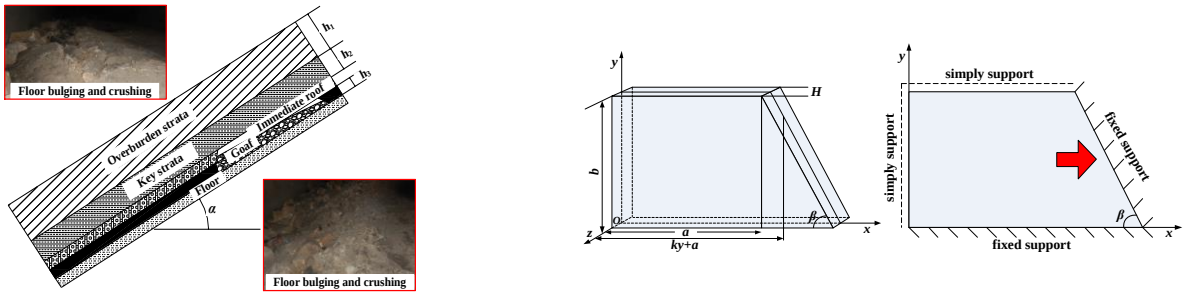

(a) Overburden strata structure model (b) Mechanical model of right angle trapezoidal stope roof

Fig. 3 Roof structure model of right angle trapezoidal stope

Table 1 Features of seam roof rocks of 10304 working face

Type	Layer	Thickness/m	Elastic modulus/GPa	Tensile strength/MPa	Poisson's ratio	Density/(kg/m^3)
Siltstone	Overburden strata	20	36	8.2	0.23	2520
Pelitic siltstone	Basic roof	5	34	7.1	0.23	2480
Mudstone	Immediate roof	6	19	5.6	0.26	2400

upper part is the return roadway. the breaking step and stress distribution of the overlying rock layer of 10304 are affected by the irregular mining face. the transport roadway of 10304 intersects with the rock gate roadway being cross-mined. As shown in Fig. 3, with the increase of excavation size, there is obvious stress concentration at the bottom of coal column. In order to reduce the degree of stress concentration in the surrounding rock of the proximity roadway, the stonegate roadway should be kept as far away as possible from the influence of the mining stress of the 10304 working face. On this basis, quantitative research can be conducted on the location of stress concentration and coal wall location to calculate the evolution characteristics of the distribution of stress in the rock surrounding rock of the stone gate roadway and provide theoretical determination of the force source for the support of the stone gate roadway.

As shown in Fig. 3(a), after 10304 working face is retrieved, the direct top of bubble falls, and part of the gangue slides or rolls downward along the inclination direction to the side of the coal wall near the unmined. As the coal wall side belongs to the solid support end, so there is no need to consider the joint action of the overlying rock layer and the gangue in the mining area. Assume that the total thickness of the overlying rock of the key layer is h_1, its average modulus of elasticity is E_1, the capacity is γ_1, Poisson's ratio is μ_1, the thickness of the hard basic top is h_2, the modulus of elasticity is E_2, the capacity is γ_2, Poisson's

ratio is μ_2, the thickness of the coal seam is h_3, the modulus of elasticity is E_3, the capacity is γ_3, Poisson's ratio is μ_3. The key layer breaking structure in Fig. 3(a) is simplified to a trapezoidal inclined elastic sheet with one side solidly supported and one side simply supported, and a mechanical model is established as shown in Fig. 3(b). Assume that the coordinate origin is located at O in the face of the model, x is the direction of pushing and mining, the length is $a+ky$, y is the direction of inclination, the length is b, and the z direction is the direction of vertical ground stress. k is the reciprocal of the inclination slope of the working face, $k=1/\tan\beta$.

The overlying seam load $P(y) = P_0-\gamma_1 \cdot y \cdot \sin\alpha$ in the direction downward along the slope of the seam. P_0 is the overlying seam load at the lower head of the working face. $P(y)$ can be decomposed into the lateral load $P_1= P(y)\cdot\cos\alpha$ perpendicular to the roof and the longitudinal load $P_2= P(y)\cdot\sin\alpha$ parallel to the roof and downward along the y-axis. The action of gravity $G = \gamma \cdot 2h_2$, horizontal constitutive force $F_1= \lambda_1 \cdot \gamma_2 \cdot h_2$, $F_2= \lambda_2 \cdot \gamma_2 \cdot h_2$ (λ_1 and λ_2 are lateral pressure coefficients) is decomposed into $G_1= G\cdot\cos\alpha$, $F_{11}= F_1\cdot\cos\alpha$ perpendicular to the roof and $F_{12}= F_1\cdot\sin\alpha$ parallel to the roof. Therefore, the key strata can be simplified as a rectangular trapezoidal thin plate under certain boundary conditions.

The deformation of the right-angle trapezoidal plate is expressed by the first-order approximate displacement function, and the deformation in the horizontal direction is expressed by the generalized beam function. The variable coefficient ordinary differential equation corresponding to the vertical displacement function under different boundary conditions is established through the principle of minimum potential energy. Solve the differential equation based on boundary conditions to obtain an analytical solution for the bending of a right angled trapezoidal plate

$$w(x, y)=u(x, y)\cdot v(y) \tag{1}$$

The displacement function in the x-direction in formula (1) is a generalized beam function in the form of simple support at one end and solid support at the other end.

$$u(x, y)=2x^4-3x^3\cdot(ky+a)+x\cdot(ky+a)^3 \tag{2}$$

The displacement in the y-direction can be solved according to the principle of minimum potential energy, and the expression of the total potential energy of the right-angle trapezoidal thin plate is

$$\Pi = -\frac{D}{2}\int_0^b\int_0^{ky+a}\left(\frac{\partial^2 w}{\partial x^2}+\frac{\partial^2 w}{\partial y^2}\right)^2 dxdy-\int_0^b\int_0^{ky+a} qw dxdy \tag{3}$$

In formula (3), q is the transverse distributed load on the roof, D is the roof flexural stiffness. The formula (1) of the right-angle trapezoidal thin roof is substituted into formula (3)

$$\Pi = -\frac{D}{2}\int_0^b\int_0^{ky+a}\begin{bmatrix}(u_{xx}+u_{yy})^2 v^2+4u_y^2 v'^2+u^2 v''^2\\ +4(u_{xx}+u_{yy})u_y vv'\\ +2(u_{xx}+u_{yy})uvv''+4u_y uv'v''\end{bmatrix}dxdy- \int_0^b\int_0^{ky+a} quvdxdy \tag{4}$$

Substitute formula (2) into formula (4) to obtain the expression for the total potential energy of the right-angle trapezoidal thin plate

$$\Pi = -\frac{D}{2}\int_0^b\begin{bmatrix}A(ky+a)^5 v^2+B(ky+a)^7 v'^2+C(ky+a)^9 v''^2\\ +E(ky+a)^8 vv'+F(ky+a)^7 vv''+G(ky+a)^8 v'v''\end{bmatrix}dy- Hq\int_0^b(ky+a)^5 vdy \tag{5}$$

Minimum potential energy when the elastic sheet is in equilibrium

$$\delta\Pi=0 \tag{6}$$

Substitute formula (5) into formula (6)

$$\begin{aligned}&(ky+a)^4 v^{(4)}+18k(ky+a)^3 v^{(3)}+\left(\frac{F-B+4kG}{C}+72k^2\right)(ky+a)^2 v''\\ &+7k\frac{F-B+4kG}{C}(ky+a)v'+\frac{A-3kE+21k^2F}{C}v=\frac{Hq}{CD}\end{aligned} \tag{7}$$

Further the variable coefficient ordinary differential equation for $v(y)$ can be obtained

$$\begin{cases}v=\left(\frac{ky+a}{kb+a}\right)^n\\ v'=n\left(\frac{k}{kb+a}\right)\left(\frac{ky+a}{kb+a}\right)^{n-1}\\ v^{(2)}=n(n-1)\left(\frac{k}{kb+a}\right)^2\left(\frac{ky+a}{kb+a}\right)^{n-2}\\ v^{(3)}=n(n-1)(n-2)\left(\frac{k}{kb+a}\right)^3\left(\frac{ky+a}{kb+a}\right)^{n-3}\\ v^{(4)}=n(n-1)(n-2)(n-4)\left(\frac{k}{kb+a}\right)^4\left(\frac{ky+a}{kb+a}\right)^{n-4}\end{cases} \tag{8}$$

Substituting the characteristic roots into formula (8) and calculating the general solution of the non-simultaneous formula (8), the bending deflection function of the right-angle trapezoidal plate can be obtained

$$\begin{aligned}&w(x,y)=u(x,y)\cdot v(y)=\left[2x^4-3x^3(ky+a)+x(ky+a)\right]\cdot\\ &\left[\begin{array}{l}\left(\frac{ky+a}{kb+a}\right)^{1.63}\left(c_1 cos\left(1.16ln\frac{ky+a}{kb+a}\right)+c_2 sin\left(1.16ln\frac{ky+a}{kb+a}\right)\right)+\\ \left(\frac{ky+a}{kb+a}\right)^{-7.63}\left(c_3 cos\left(1.25ln\frac{ky+a}{kb+a}\right)+c_4 sin\left(1.25ln\frac{ky+a}{kb+a}\right)\right)+0.02\frac{q}{D}\end{array}\right]\end{aligned} \tag{9}$$

Based on the conditions of long-side solid support and short-side simple support, the boundary conditions of right-angle trapezoidal thin-slab rock formation

$$\begin{cases}v(y)\big|_{y=b}=0\\ \left.\frac{\partial v}{\partial y}\right|_{y=b}=0\\ v(y)\big|_{y=0}=0\\ \left[(ky+a)^2 v''+9(ky+a)v'\right]_{y=0}=0\end{cases} \tag{10}$$

Substituting formula (9) into formula (10), the stress state at each point of the key strata of the right-angle trapezoidal thin plate is obtained

$$\begin{cases}\sigma_x=-\frac{Ez}{1-\mu^2}\left(\frac{\partial^2 w}{\partial x^2}+\mu\frac{\partial^2 w}{\partial y^2}\right)\\ \sigma_y=-\frac{Ez}{1-\mu^2}\left(\frac{\partial^2 w}{\partial y^2}+\mu\frac{\partial^2 w}{\partial x^2}\right)\\ \tau_{xy}=-\frac{Ez}{1+\mu}\frac{\partial^2 w}{\partial x\partial y}\\ \tau_{xz}=\frac{E}{2(1-\mu^2)}\left(z^2-\frac{h^2}{4}\right)\frac{\partial}{\partial x}\nabla^2 w\\ \tau_{yz}=\frac{E}{2(1-\mu^2)}\left(z^2-\frac{h^2}{4}\right)\frac{\partial}{\partial y}\nabla^2 w\end{cases}$$

Table 2 Statistical results of key strata breaking steps

Key strata	The first strata of siltstone		The third strata of siltstone	
Breaking parameter	Breaking step at the end of the upper surface/m	Breaking step in the middle of the lower surface/m	Breaking step at the end of the upper surface/m	Breaking step in the middle of the lower surface/m
First breaking	49	58	39	49
Second breaking	51	57	38	47
Third breaking	52	53	39	44

2.2 Key strata breaking characteristics

The roof has two forms of damage, which are the overall shear damage along the coal wall and the tensile damage in the middle of the roof plate. In order to avoid the damage to personnel or equipment caused by the large incoming pressure strength of the roof shear damage, the roof should be as much as possible to show the progressive tensile breakage. According to the maximum shear stress theory of the top plate boundary damage judgment of the overall shear, the minimum value of the top plate boundary in the four limit push progress distance is the critical push progress distance of the top plate shear breakage. Based on the maximum tensile stress theory, the limit pushing distance of the trapezoidal top plate for progressive tensile damage can be calculated and compared with the critical pushing distance of the top plate for shear breakage, and the minimum value of the two is the limit pushing distance of the trapezoidal top plate for breakage.

The breaking sequence of the overlying rock layer on the roof depends on the number of breaking steps of each rock layer, independent of the inclination length of the working face. Calculate the load of the key layer based on the deformation characteristics of the key layer

$$q_1 = \frac{E_1 h_1^3}{1-\nu_1^2} \sum_{i=1}^{n} \rho_1 g h_i \Big/ \sum_{i=1}^{n} \frac{E_i h_i^3}{1-\nu_i^2} \tag{12}$$

According to formula (12), q_{11} = 0.055 MPa, q_{12} = 0.18 MPa, and q_{13} = 0.079 MPa. Since $q_{11} < q_{12} > q_{13}$, the siltstone of the first layer and the siltstone of the third layer can be judged as critical layers. Considering the mechanical model of 10304 right-angle trapezoidal quarry roof in which the long side is the solid support end and the short side is the simple support end. Therefore, the tensile breakage criterion of the critical layer can be used to calculate the ultimate breakage step and ultimate overhanging area of the first layer of siltstone and the third layer of siltstone respectively, and then determine the main critical layer and sub-critical layer.

According to the calculation results of the key layer breakage step counted in Table 2, the breakage step of the third siltstone is smaller than that of the first siltstone, which indicates that the third siltstone and the first siltstone will form a composite key layer and move together.

Due to the slanting advance of 10304 working face, the peak of over-support pressure affects the surrounding rock deformation of cross-mining roadway in sections, avoiding the concentration of over-support pressure acting on cross-mining roadway in the same time. According to the field measurement results, the initial collapse step during the working face advance is 52 m, and the periodic collapse step is 18 m, the peak of overrunning support pressure is located about 10 m in front of the coal wall of the working face, and the bottom plate of the roadway is in the periodic pressure stage during the cross-mining.

3. Transmission characteristics of mining stress in floor

In the process of coal seam mining, the stress balance around the quarry is broken and leads to the dynamic evolution of the surrounding rock stress, while forming stress-raising and stress-lowering areas, which in turn affects the stability of the surrounding rock of the roadway. In order to reduce the impact of mining stress on the roadway and protect the safety of personnel and equipment inside the roadway, the analysis should focus on the characteristics of mining stress distribution and transmission law to avoid the cross-mining roadway is located in the peak impact area of mining stress. Therefore, by studying the distribution characteristics of mining stress in trapezoidal quarry and its transmission mechanism in the surrounding rock, it can provide a theoretical basis for realizing the active control of the roadway.

3.1 Distribution characteristics of mining stress

The over-supported mining dynamic stress is formed in front of the working face during coal seam mining and is parallel to the mining face after adjusting the slope. Therefore, getting the shear stress distribution of the top plate boundary of the quarry can determine the load borne by the coal column, and then obtain the stress distribution

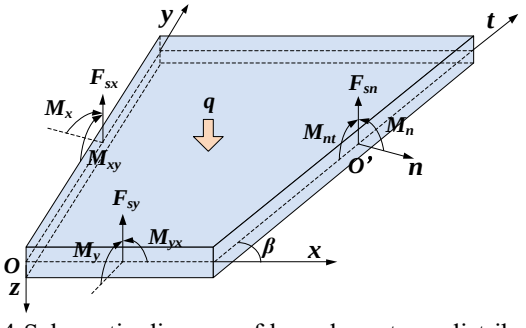

Fig. 4 Schematic diagram of boundary stress distribution of right angle trapezoidal key strata

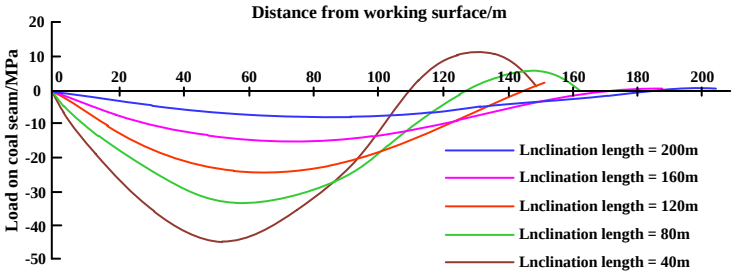

Fig. 5 Load evolution characteristics of coal pillar in front of working face

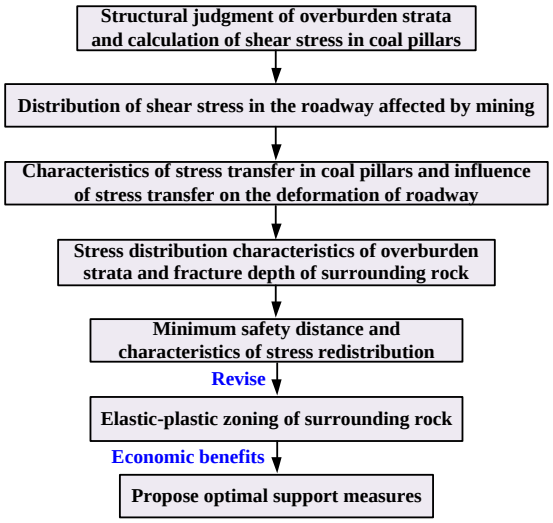

Fig. 6 Flow chart for calculating the rupture depth of surrounding rock affected by mining

characteristics of the roadway envelope that changes with the distance from the mining face. The load distribution of the right-angle trapezoidal key seam boundary is shown in Fig. 4.

The bending moments M_x and M_y and the torques Mxy on the right-angle sides are

$$\left.\begin{aligned} M_x &= -D\left(\frac{\partial^2 w}{\partial x^2}+\mu\frac{\partial^2 y}{\partial y^2}\right) \\ M_y &= -D\left(\frac{\partial^2 w}{\partial y^2}+\mu\frac{\partial^2 w}{\partial x^2}\right) \\ M_{xy} &= M_{xy} = -D(1-\mu)\frac{\partial^2 w}{\partial x \partial y} \end{aligned}\right\} \tag{13}$$

The shear force F_{sx} and F_{sy} are

$$\left.\begin{aligned} F_{Sx} &= \frac{\partial M_x}{\partial x}+\frac{\partial M_{yx}}{\partial y} \\ F_{Sy} &= \frac{\partial M_y}{\partial y}+\frac{\partial M_{yx}}{\partial x} \end{aligned}\right\} \tag{14}$$

Further find the bending moment M_n, torque M_{nt}, shear force F_{sn}

$$M_n = M_x \cos^2\alpha + M_y \sin^2\alpha + M_{xy}\sin 2\alpha \tag{15}$$

$$M_{nt} = M_{xy}\cos 2\alpha + \frac{1}{2}(M_x - M_y)\sin 2\alpha \tag{16}$$

$$F_{sn} = F_{sx}\cos\alpha + F_{sy}\sin\alpha \tag{17}$$

With the distance from the working face shortened, the peak load above the coal and its increasing rate both showed an increasing trend. Among them, at 100 m from the working face, the load on the oblique side of the coal column of the right-angle trapezoidal quarry is 43 MPa, the load on the short side of the coal column is 33 MPa, and the load on the vertical side of the coal column is 13 MPa, which indicates that the right-angle trapezoidal thin plate solid support boundary is more prone to surrounding rock stress concentration compared with the simple support boundary. In addition, with the pushing of the working face, the peak coal load position gradually shifts to the interior of the quarry (Fig. 5).

The main influencing factors of cross-mining roadway stability include safety distance, inclination angle of coal seam, coal seam thickness and quarry size. In order to achieve safe and efficient cross-mining, the influence of mining stress on the stability of the roadway must be studied in detail to provide a theoretical basis for the proposed cross-mining roadway support method. The process of calculating the fracture depth of surrounding rock affected by mining stress during the pushing of trapezoidal working face is shown in Fig. 6.

According to the calculation process in Fig. 6, the overlying rock transport characteristics of the quarry are taken as the carrier of the coal body, and the load

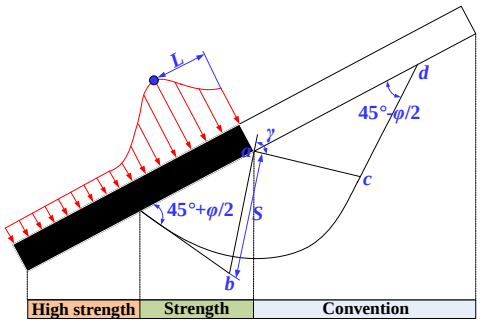

Fig. 7 Schematic diagram of floor failure depth and zoning support

transferred to the bottom plate of the roadway is obtained by calculating the shear stress of the coal body, and the minimum safety distance is determined according to the elastic-plastic partition of the surrounding rock and the influence range of the mining stress. At the same time, according to the vertical distance of the quarry floor from the roadway and the stress state of the surrounding rock, the roadway is divided into different sections and the stability analysis is carried out separately.

As shown in Fig. 7, the damage depth of the roadway bottom slab can be determined according to the ultimate bearing formula of the taishaji foundation (Zhou *et al.* 2002).

$$r = arcsin\frac{1-m+(3+m)sin\varphi}{3+sin\varphi} \tag{18}$$

$$s = \frac{L}{2cos(45+\varphi/2)} \tag{19}$$

In formula (18), m is the intermediate principal stress parameter, $m=2\sigma_2/(\sigma_1+\sigma_3)$, φ is the internal friction angle of the rock, S is the length of ab, and L is the distance between the peak support pressure and the coal body.

The boundary bc can be expressed as a logarithmic spiral curve

$$s_1 = s\,exp\{\theta\times\frac{1-m+(3+m)sin\varphi}{\sqrt{(3+sin\varphi)^2-[1-m+(3+m)sin\varphi]^2}}\} \tag{20}$$

In formula (20), s_1 is any vector diameter, s is the starting vector diameter, and θ is the angle between s_1 and s. Combined formulas (18)-(20) can determine the depth of damage of the bottom plate caused by the support pressure at the working face V_1

$$V_1 = \frac{L\,sin(\theta-45+\varphi/2)}{2cos(45+\varphi/2)}exp[(45+\varphi/2)tan\varphi] \tag{21}$$

3.2 Analysis of floor failure characteristics

Taking the mining of 10304 cross-mining face of Zhongheng coal mine as the engineering background, the numerical simulation method of granular flow is used to establish the mining field model, to study the breaking law of the right-angle trapezoidal thin plate key layer under

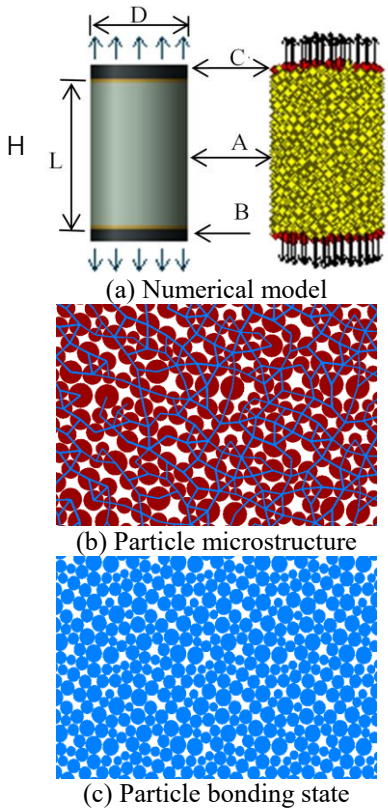

(a) Numerical model

(b) Particle microstructure

(c) Particle bonding state

Fig. 8 Numerical model for rock parameter calibration

Table 3 Microproperties parameters of rock

Element	Parameter	Value
Ball	Minimum radius/m	6.7×10^{-2}
	Particle size ratio	1.5
	Density/(g/cm^3)	2.63
Contact	Contact modulus/GPa	37
	Stiffness ratio	2.46
	Friction coefficient	0.5
Bond	Average normal strength/ Standard deviation(MPa)	30/0
	Average tangential strength/ Standard deviation(MPa)	40/0
	Elastic modulus/GPa	37
	Stiffness ratio	2.46
	Radius multiplier	1

different advancing distance conditions and its influence characteristics on the coal body bearing, and to compare with the theoretical analysis results, and then to provide a reasonable basis for the design of the field section.

In order to ensure that the particle flow simulation procedure can be applied efficiently in engineering problems, a direct tensile test model at large particle size is established with the help of PFC2D software and the built-in FISH language and its algorithm to realize the calibration of rock parameters for this simulation. A cylindrical specimen is used for the direct tensile test, and its test model and numerical model of particle flow are shown in Fig. 8.

Table 4 Meso-parameters of overlying stratum of 10304 workface

Strata	Microscopic parameters					Macro parameters			
	E_c /GPa	K_n/K_s	μ	σ_c /MPa	τ_c /MPa	E /GPa	v	σ_c /MPa	τ_c /MPa
Coal	20	2	0.6	5	8	23.7	0.21	17.43	3
Siltstone	40	1.5	0.5	10	16	54.1	0.17	18.93	14
Mudstone	35	1.8	0.4	12	15	76.7	0.21	10.8	13

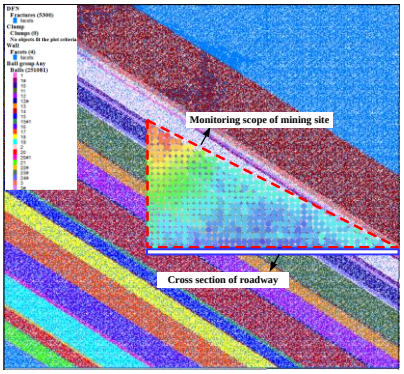

Fig. 9 Numerical model for rock parameter calibration

In Fig. 8, A is a rock specimen with height H and diameter D, and B is a resin cementation layer, which is replaced by a high adhesive strength (adhesion of red and yellow parts) in the numerical model. Table 3 counts the numerical model fine view parameters, where the value of end bond strength is 10 times of rock bond strength, and the rest parameters are the same as rock. Table 4 counts the fine-view parameters of the overlying rock layer of Zhongheng coal mine 10304.

The structure of the numerical model is shown in Fig. 9, which mainly simulates the stress distribution characteristics of the top and bottom slab of the roadway after mining the coal seam above the roadway, where the thickness of the coal seam is 3.5 m and the thickness of the key layer above the coal seam is 28 m. The upper rock layer of the key layer is replaced by a uniform load q = 3.5 MPa. The particle range is 0.6-0.7 m, the particle size values obey Gaussian distribution, and a total of 251801 particles are generated. The red dashed line in Fig. 8 shows 463 monitoring points arranged in the top and bottom of the roadway, the coal seam above the roadway and the key layer, and the profile of the cross-mining roadway is within the blue solid line below the monitoring points.

Fig. 10 shows the fracture development characteristics of the surrounding rock under different pushing distance conditions. The red color represents that the rock is under pressure and the blue color represents that the rock is under tension. After pushing 45 m, the development of fissures in the surrounding rock of the roadway is obvious, indicating that the location of the roadway is affected by the adopted stress. When the working face was pushed to 90 m, the development of fissures in the surrounding rock of the roadway further increased, indicating that the mining stress disturbance can accelerate the development of fissures in the surrounding rock. When the cross-mining is finished,

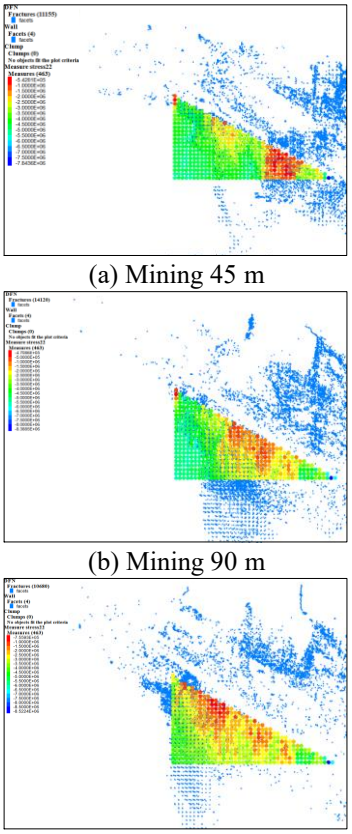

(a) Mining 45 m

(b) Mining 90 m

(c) Mining 135 m

Fig. 10 Characteristics of surrounding rock fracture under different mining lengths

the direct top collapse, the surrounding rock fissure area continues to develop to the deep on the original basis, and the channel surrounding rock fissure area is on the rising trend, forming a typical interlaced fissure zone. The comprehensive study found that the fissure expansion speed is faster at the early stage of mining, and the fissure expansion speed slows down gradually with the increase of pushing mining distance. In addition, the laminar structure of fissure expansion is obvious, all of them develop from the mining place to both ends.

As shown in Fig. 11, the influence range of mining stress moves with the change of pushing mining distance. After pushing 45 m, the stress in the surrounding rock of the roadway rises rapidly, which means that the overrun mining stress is transferred to the location of the roadway through the coal seam, and at this time, the range affected by mining stress is the smallest, but the concentration of stress in the surrounding rock is the highest. When the working face is

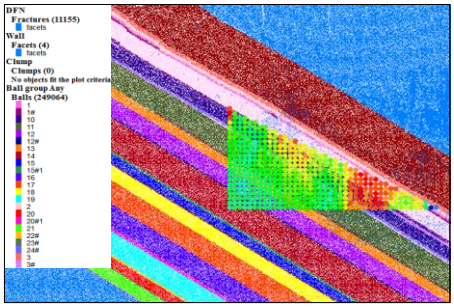

(a) Mining 45 m

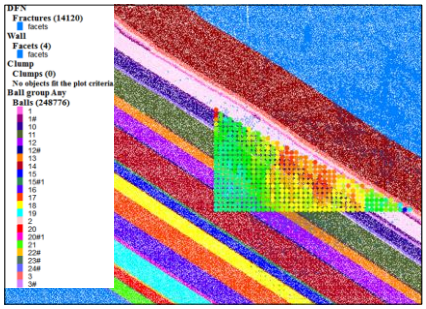

(b) Mining 90 m

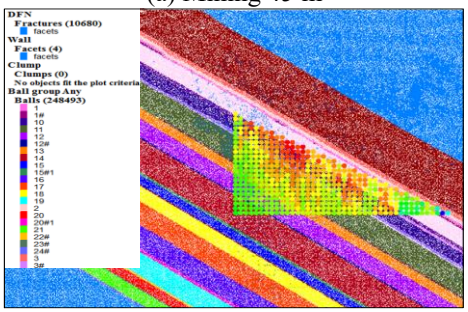

(c) Mining 135 m

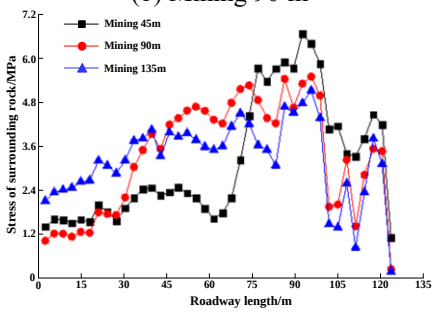

(d) Stress distribution curve of surrounding rock

Fig. 11 Characteristics of surrounding rock stress under different mining lengths

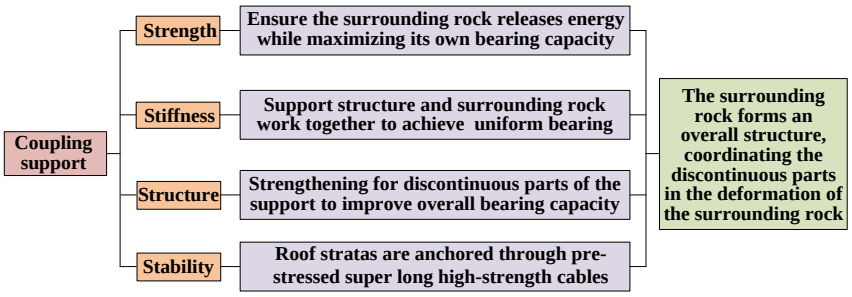

Fig. 12 Main characteristics of coupled support

pushed to 90 m, the peak stress in the surrounding rock of the roadway decreases and the influence range of mining stress expands. The peak stress decrease is mainly caused by the increase of vertical distance between the working face and the roadway and the gradual decay of stress transmission. The main reason for the expansion of the influence range of mining stress is the continuous transport of the overlying rock layer. The mining stress influence range at the end of cross-mining is the largest, and the stress concentration in the surrounding rock is the lowest. In addition, the range of mining influence in different sections of the roadway varies, but the trend of the change of the surrounding rock stress is basically the same, and the overall evolution of the surrounding rock stress with the change of the pushing distance is slowly rising and then slowly decreasing, which indicates that the mining stress at the working face and the cross-mining roadway mine pressure is not positively correlated.

4. Support method for overhead mining roadway

According to the numerical simulation results of cross-mining roadway, there are three main factors affecting the stability of cross-mining roadway, one is the excessive development of fissures in the surrounding rock of cross-mining roadway, which reduces the bearing capacity of the surrounding rock itself, the second is the formation of pressure relief space in the cross-mining roadway section, which easily causes the expansion and deformation of the top and bottom plates and the two helpers, and the third is the periodic fracture of the overlying rock layer with the pushing of the working face, which gradually releases the stress of the surrounding rock to the roadway and forms a fracture zone. In view of the above influencing factors, it is necessary to propose different support methods based on the principles of overall design, timely support, high-strength support and coupling support, according to different locations of the cross-mining roadway, and control the deformation of the surrounding rock of the cross-mining roadway through the double coupling of active support structure and surrounding rock, and active support structure and passive support structure coupling (Fig. 12).

As shown in Fig. 13, based on the numerical simulation results of the stress distribution in the surrounding rock of the cross-mining roadway, the cross-mining roadway is divided into three zones, such as ordinary support, enhanced

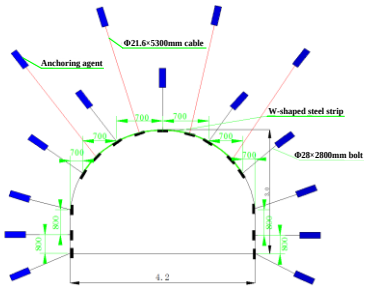

(a) Convention

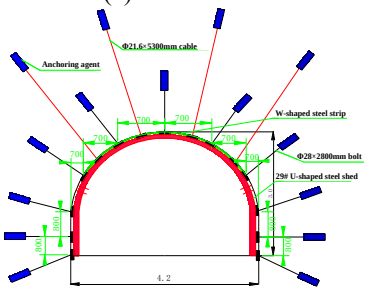

(b) Strength

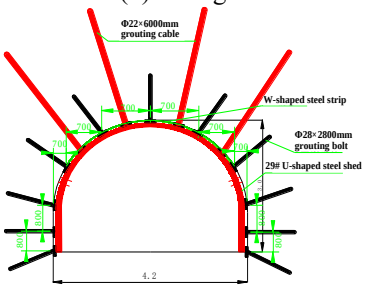

(c) High strength

Fig. 13 Schematic diagram of roadway cross-section support

Table 5 Characteristics of basic suppor

Type	Size/mm	Spacing/mm
Bolt	Φ28×L2800(roof) Φ28×L2800(sides)	700×900 800×900
W-shaped steel strip	3800×183×5	750
Steel mesh	2400×900	100×100
Cable	Φ21.6mm×L5300 (Non grouting)	1500×1500

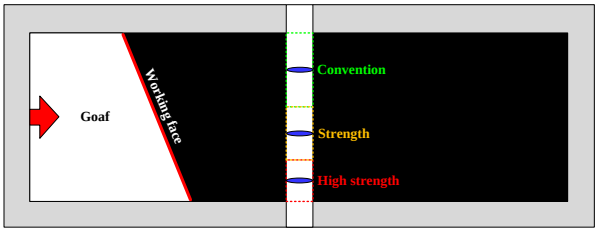

(a) Schematic diagram of monitoring location

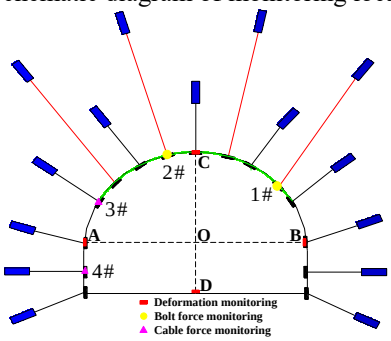

(b) Section monitoring

Fig. 14 Layout diagram of stress and deformation monitoring monitoring

support and key support, etc. Based on active support, the corresponding passive support method is selected according to the different surrounding rock stress conditions. The basic parameters of active support structure are statistically presented in Table 5.

(1) Active coupling support structure with non-grouted anchor cables is used in the general support area. The anchor cable diameter is 21.6 mm, the length is 5300 mm, and the inter-row distance is 700 mm × 2000 mm.

(2) The active coupling support structure of non-grouted anchor cable + passive support structure of U-shaped steel shed is adopted in the reinforced support area. Among them, the U-shaped steel shed is U29, and the spacing of U-shaped steel shed is 2000 mm. the diameter of anchor cable is 21.6 mm, the length is 5300 mm, and the distance between rows is 700 mm × 1500 mm.

(3) The key support area adopts the active coupling support structure of grouted anchor cable + passive support structure of U-shaped steel shed, forming a linkage double coupling support system. Among them, the U-shaped steel shed is U29, and the spacing of U-shaped steel shed is 1000 mm. the diameter of slurry anchor cable is 22 mm, the length is 6000 mm, the inter-row distance is 700 mm × 1000 mm, and the maximum slurry depth is 7000 mm.

Cross-mining roadway deformation is mainly affected by the mining stress of irregular working face, so it is necessary to monitor the amount of surrounding rock deformation as well as the force of the supporting structure in the cross-mining roadway after the support of zoning section. As shown in Fig. 14, measurement points are arranged at 100m from the working face respectively. The deformation of the surrounding rock in the measurement point is monitored by the cross-point method, while the anchor cable and anchor rod forces are monitored by the mine MSJ-202 vibrating string anchor cable force gauge and the mine SDMG-75 anchor rod force gauge, respectively.

The monitoring results of the deformation of the roadway surrounding rock are shown in Fig. 15, and the monitoring results of the anchor rod and anchor cable force are shown in Fig. 16. The amount of top and bottom slab shifting in the section of ordinary support, reinforced support and key support is significantly larger than the deformation amount of the two gangs. Among them, the maximum amount of top plate sinking is 170 mm, and the maximum amount of bottom plate bulging is 50 mm, the deformation is within the allowable range of cross-mining roadway. In addition, the force of anchor cable and anchor rod increased with the decrease of distance from the working face. The maximum force of top plate anchor cable in the key support section was 170 kN, the maximum force of anchor cable in the gang was 155 kN, and the maximum

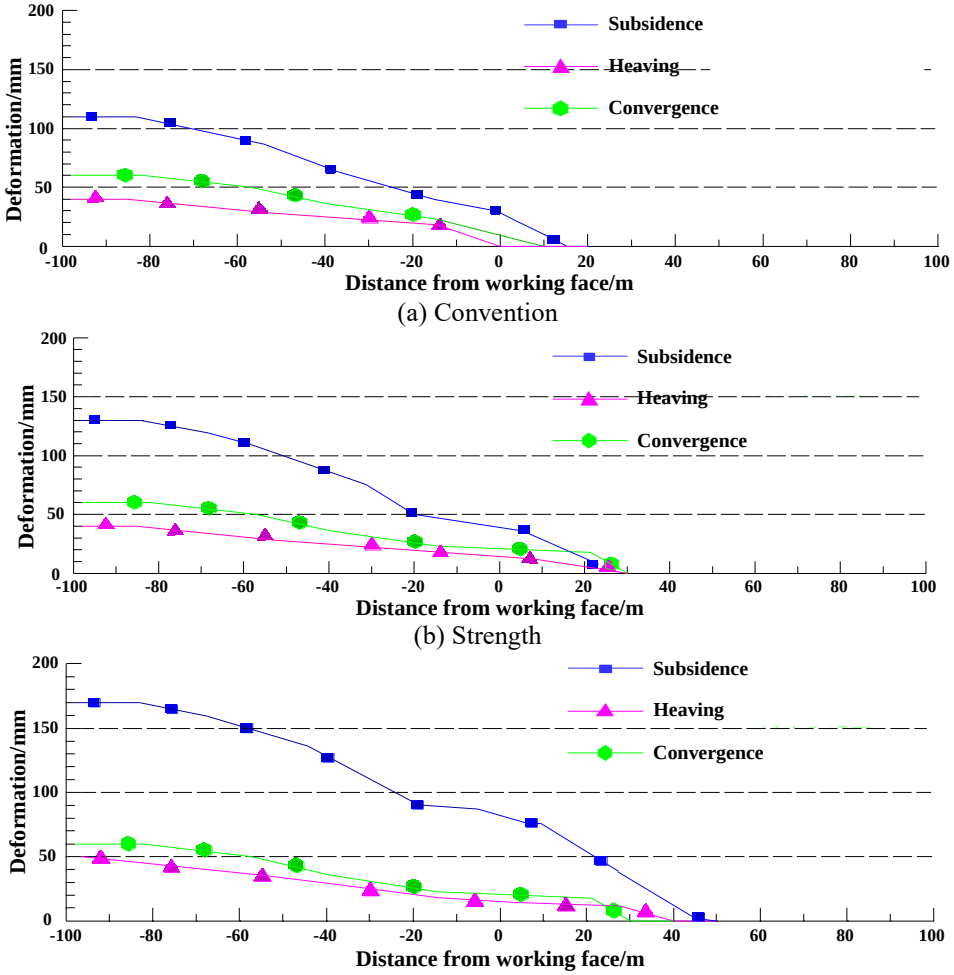

(a) Convention

(b) Strength

(c) High strength

Fig. 15 Deformation of surrounding rock at different distances from the working face

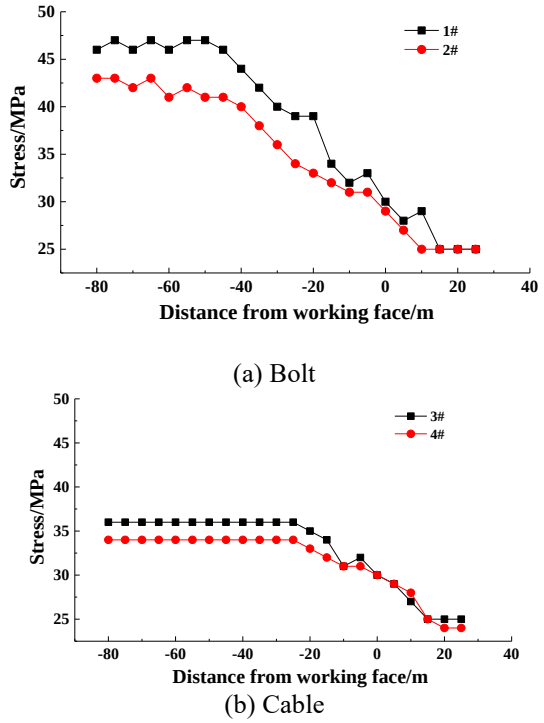

(a) Bolt

(b) Cable

Fig. 16 Support stress at different distances from the working face

force of anchor rod was 98 kN, which were all within the anchorage range. It means that the anchor rod and anchor cable are selected appropriately and the double coupling support method achieves the expected goal.

5. Discussion

Considering that the top plate breaking has an important influence on the stress transfer of the surrounding rock, it is important to study the destabilization process and breaking law of the right-angle trapezoidal thin plate to guide the support of the cross-mining roadway. As shown in Fig. 17, the shear stress evolution characteristics of the right-angle trapezoidal roof slab boundary are illustrated by pushing 150 m of the working face as an example, and the selected shear stress values are all located at the middle face of the rock layer.

According to the analysis of shear stress distribution characteristics, the reverse shear stress is distributed at the endpoints of the right-angle trapezoidal quarry boundary. The analysis of its principle is mainly due to the stress concentration at the endpoints of the trapezoidal roof boundary, when subjected to lateral load, there is a tendency

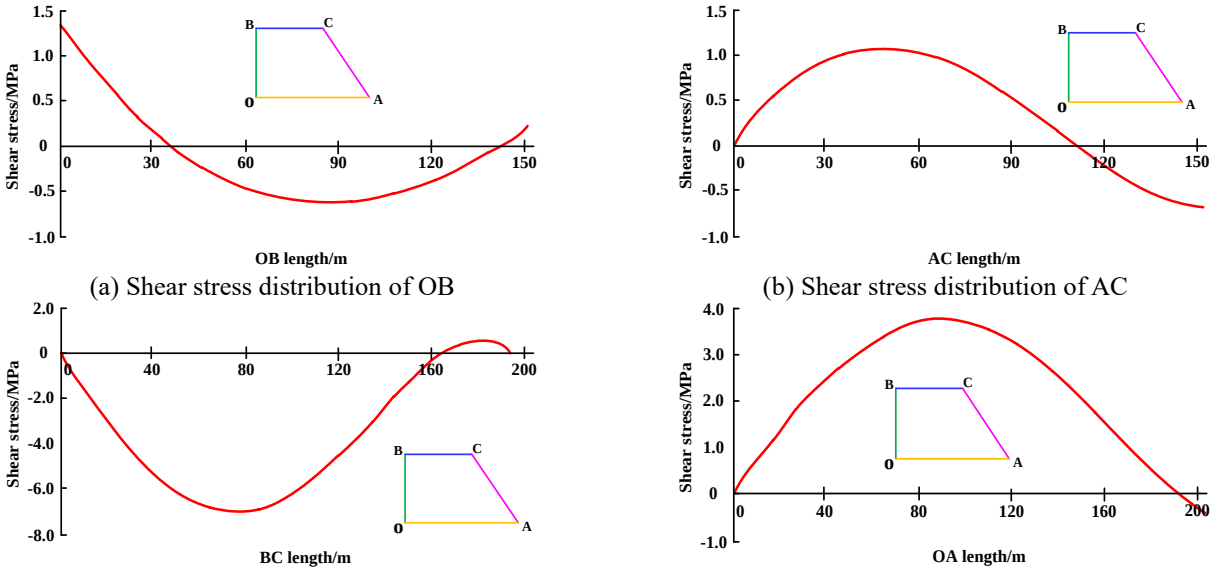

(a) Shear stress distribution of OB

(b) Shear stress distribution of AC

(c) Shear stress distribution of BC

(d) Shear stress distribution of OA

Fig. 17 Support stress at different distances from the working face

of upturning at the endpoints, but affected by the vertical downward reaction force. oB side and AC side and BC side and OA side, the shear stress distribution on the opposite sides is basically opposite, indicating that the top plate is in balance. peak shear stress on OA side (7.2 MPa) > peak shear stress on BC side (4 MPa) > peak shear stress on OB side (1.3 MPa) > peak shear stress on AC side (0.8 MPa). OB side peak shear stress (1.3 MPa) > AC side peak shear stress (0.8 MPa), analyze the reason, BC side and OA side length is much larger than OB side and AC side, BC side and OA side bear more load, but BC side is simple support structure, OA side is solid support structure, therefore, OA side peak shear stress is higher than BC side. In addition, the peak shear stresses at the boundary of the trapezoidal top slab are all located near the middle of the boundary, indicating that the peak support pressure on the coal body is also located near the middle of the boundary.

With the above analysis, when the key layer of right-angle trapezoidal sheet breaks, the damage occurs first from the solid support edge of the upper surface of the rock layer, and with the pushing of the working face, the tensile damage occurs in the middle of the lower surface of the rock layer and leads to the crack penetration of the upper and lower surfaces of the rock layer, and the key layer breaks and destabilizes as a whole. Therefore, the limit pushing progress distance of the quarry should be the quarry pushing progress distance when tensile damage occurs in the middle of the lower surface of the rock formation.

As shown in Fig. 18, the slope k of the right-angle trapezoidal slope is set in the range of -0.9 - 0.9, and the effect of k on the maximum tensile stress in the middle of the lower surface of the rock formation is studied. When k < 0, the maximum tensile stress of the formation increases exponentially with the decrease of the slope, and the formation breaks and destabilizes after exceeding the tensile strength. When k > 0, the maximum tensile stress of the

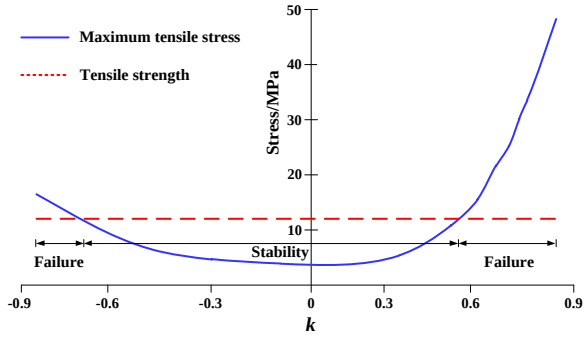

Fig. 18 Curve of maximum tensile stress changing with *k*

rock layer increases exponentially with the increase of slope, and the growth rate is greater than when k < 0. When k > 0.6, the rock layer breaks and destabilizes because it reaches the tensile strength. It means that when the slope of the right-angle trapezoidal roof slope exceeds its limit, the rock formation breaks and destabilizes, so k should be set in the stable range when adjusting the mining parameters.

6. Conclusions

(1) The model of key layer of right-angle trapezoidal thin plate is established by using elastic thin plate theory, and the analytical solution of bending and sinking of key layer of right-angle trapezoidal thin plate with two sides solid support and two sides simple support is obtained by using Kantorovich method, and the criterion of shear and tensile rupture instability of key layer is given, according to which the limit pushing progress distance and limit overhanging area of right-angle trapezoidal quarry are calculated.

(2) The fissures in the surrounding rock of the roadway gradually develop from shallow to deep and approximately develop in an elliptical funnel shape in all directions, within

the range of rock layers pushed by the trapezoidal quarry, the dominant direction of the fissures in the surrounding rock is horizontal development along the rock layer, and the fissures in the non-mining rock layer are mainly vertical development. The fissure development in the non-mining rock layer is mainly in vertical direction.

(3) Based on the theoretical calculation of the maximum depth of surrounding rock failure and the minimum safe coal rock column spacing, the cross mining roadway is divided into key support areas, strengthened support areas, and ordinary support areas. Through the proposed dual coupling support method of active and passive combination, the maximum force of the roadway anchor cable is 170 kN, and the maximum force of the anchor rod is 98 kN.

(4) This stdy focuses on the overlying rock layers and size distribution of the working face, simplifying the key layer into thin plates for research. But the thickness of the overlying rock layer is not constant, but shows dynamic changes. Subsequent research should focus on the overall movement of the impact range of the key layers of the irregular plate in real-time state.

Acknowledgements

The research described in this paper was financially supported by National Natural Science Foundation of China (Nos. 52304136, 51974358 and 52104239), Natural Science Foundation of Chongqing (CSTB2022NSCQ-MSX1080 and cstc2020jcyj-msxmX1052).

References

Chen, L., Gao, S.Y., Miao, B., Yao, N., Zhang, S.Z. and Zhang, W. (2022), "Field detection and numerical simulation study on roof asymmetric fracture mechanism of large-span soft rock roadway with discontinuity surface", *Geofluids*, **2022**, 8945239. https://doi.org/10.1155/2022/8945239.

He, J.H., Li, W.P., Liu, Y., Yang, Z., Liu, S.L. and Li, L.F. (2018), "An improved method for determining the position of overlying separated strata in mining", *Eng. Fail. Anal.*, **83**, 17-29. https://doi.org/10.1016/j.engfailanal.2017.09.015.

Liu, H.L., Zhao, Y., Zhang, P.H., Liu, F.Y. and Yang, T.H. (2021), "Stope structure evaluation based on the damage model driven by microseismic data and Mathews stability diagram method in Xiadian gold mine", *Geomat. Nat. Haz. Risk*, **12**(1), 1616-1637. https://doi.org/10.1080/19475705.2021.1941308.

Liu, X., Tu, S.H., Tu, H.S., Tang, L., Ma, J.Y., Li, Y., Li, W.L., Miao, K.J. and Tian, H. (2023), "Numerical simulation study on stability control technology of Large-Area Wall Caving Area (LAWCA) in large-inclined face", *Geofluids*, **2023**, 5352974. https://doi.org/10.1155/2023/5352974.

Ma, K., Yang, T.H, Zhao, Y., Hou, X.G., Liu, Y.L., Hou, J.X., Zheng, W.X. and Ye, Q. (2022), "Mechanical model for analyzing the water-resisting key stratum to evaluate water inrush from goaf in roof", *Geomech. Eng.*, **28**(3), 299-311. https://doi.org/10.12989/gae.2022.28.3.299.

Meng, G.H., Zhang, J.X., Li, M., Wang, C.J., Zhou, N. and Zhang, L.B. (2023), "Bearing characteristics and safety control of hydraulic support groups in shallow-buried thin bedrock ultra-long working faces", *J. Cent. South Univ.*, **30**(5), 1662-1674. https://doi.org/10.1007/s11771-023-5313-9.

Pan, W.D., Deng, C., Yang, Y.C., Zhang, K.M. and Gao, S. (2022), "Pressure law of roof and supporting technology of roadway when working face passing through abandoned roadway", *Shock Vib.*, **2022**, 7565629. https://doi.org/10.1155/2022/7565629.

Shan, R.L., Li, Z.L., Wang, C.H., Wei, Y.H., Tong, X., Liu, S. and Shan, Z.H. (2021), "Study on the distribution characteristics of stress deviator in the surrounding rock when mining closely spaced coal seams", *Environ. Earth Sci.*, **80**(17), 602. https://doi.org/10.1007/s12665-021-09891-1.

Tian, M.L., Gao, X.X., Zhang, A.F., Han, L.J. and Xiao, H.T. (2024), "Study on the deformation failure mechanism and coupling support technology of soft rock roadways in strong wind oxidation zones", *Eng. Fail. Anal.*, **156**, 107840. https://doi.org/10.1016/j.engfailanal.2023.107840.

Wang, C.L., Li, G.Y., Gao, A.S., Shi, F., Lu, Z.J. and Lu, H. (2021), "Optimal pre-conditioning and support designs of floor heave in deep roadways", *Geomech. Eng.*, **14**(5), 429-437. https://doi.org/10.12989/gae.2018.14.5.429.

Wang, J.C., Liu, F. and Zhang, J.W. (2019), "Investigation on the propagation mechanism of explosion stress wave in underground mining", *Geomech. Eng.*, **17**(3), 297-307. https://doi.org/10.12989/gae.2019.17.3.297.

Wang, Q., Jiang, Z.H., Jiang, B., Gao, H.K., Huang, Y.B. and Zhang, P. (2020), "Research on an automatic roadway formation method in deep mining areas by roof cutting with high-strength bolt-grouting", *Int. J. Rock Mech. Min.*, **128**, 104264. https://doi.org/10.1016/j.ijrmms.2020.104264.

Wang, Z.K., Li, W.P., Wang, Q.Q., Hu, Y.B. and Du, J.F. (2021), "Monitoring the dynamic response of the overlying rock-soil composite structure to underground mining using BOTDR and FBG sensing technologies", *Rock Mech. Rock Eng.*, **54**(9), 5095-5116. https://doi.org/10.1007/s00603-021-02530-y.

Wen, Y.Y., Cao, A.Y., Guo, W.H., Xue, C.C., Lv, G.W. and Yan, X.L. (2023), "Strata movement and mining-induced stress identification for an isolated working face surrounded by two goafs", *Energies*, **16**(6), 2839. https://doi.org/10.3390/en16062839.

Wu, K.B., Zou, J.P., Jiao, Y.Y., He, S.J. and Wang, G.M. (2023), "Insight and effectiveness of working-face deep-hole blasting for prevention of strong seismicity induced by deep coal mining", *Rock Mech. Rock Eng.*, **56**(12), 8693-8709. https://doi.org/10.1007/s00603-023-03516-8.

Xiong, Y., Kong, D.Z., Song, G.F. and He, Y. (2024), "Failure mechanism and 3D physical modeling test of coal face pyramid sliding in steeply inclined working face: A case study", *Eng. Fail. Anal.*, **159**, 108064. https://doi.org/10.1016/j.engfailanal.2024.108064.

Xu, Y.L., Pan, K.R. and Zhang, H. (2019), "Investigation of key techniques on floor roadway support under the impacts of superimposed mining: theoretical analysis and field study", *Environ. Earth Sci.*, **78**(15), 436. https://doi.org/10.1007/s12665-019-8431-9.

Yang, S.G., Xu, N., Liu, H.X., Zhang, X.F. and Mei, S.X. (2024), "Research and application of 'three zones' range within overlying strata in goaf of steep coal seam", *Front. Energy Res.*, **12**, 1333016. https://doi.org/10.3389/fenrg.2024.1333016.

Yang, Z.Q., Liu, C., Zhu, H.Z., Xie, F.X., Dou, L.M. and Chen, J.H. (2019), "Mechanism of rock burst caused by fracture of key strata during irregular working face mining and its prevention methods", *Int. J. Min. Sci. Techno.*, **29**(6), 889-897. https://doi.org/10.1016/j.ijmst.2018.07.005.

Zhang, J., Wang, B., Bai, W.Y. and Yang, S. (2021), "A study on the mechanism of dynamic pressure during the combinatorial key strata rock column instability in shallow multi-coal seams", *Adv. Civ. Eng.*, 6664487. https://doi.org/10.1155/2021/6664487.

Zhang, W., Zhao, T.B. and Zhang, X.T. (2023), "Stability analysis and deformation control method of swelling soft rock roadway adjacent to chambers", *Geomech. Geophys. Geo.*, **9**(1), 91. https://doi.org/10.1007/s40948-023-00635-y.

Zhao, S.K., Sui, Q.R., Cao, C., Wang, X.C., Wang, C.L., Zhao, D.M., Wang, Y. and Zhao, Y. (2021), "Mechanical model of lateral fracture for the overlying hard rock strata along coal mine goaf", *Geomech. Eng.*, **27**(1), 75-85. https://doi.org/10.12989/gae.2021.27.1.075.

Zhou, X.P., Huang, Y.B. and Ding, Z.C. (2002), "Influence of intermediate principal stress on the formula of Terzaghi ultimate beating capacity of foundations", *Chinese J. Rock Mech. Eng.*, **21**(10), 1554-1556. https://doi.org/10.3321/j.issn:1000-6915.2002.10.025.

CC